Knockdown of miR-411-3p induces M2 macrophage polarization and promotes colorectal cancer progression by regulation of MMP7

Tianliang Bai,[1#] Ping Li,[1#] Yabin Liu,[2] Bindan Cai,[3] Gang Li,[1] Wenbin Wang,[1] Rui Yan,[1] Xiangkui Zheng,[1] Shangkun Du[1]

[1]Department of Gastrointestinal Surgery, Affiliated Hospital of Hebei University, Baoding, Hebei Province
[2]Department of General Surgery, Fourth Hospital of Hebei Medical University, Hebei Province
[3]Department of Neurology, Zhuozhou City Hospital, Hebei Province, China

[#]*These authors share first authorship as they equally contributed to this work.*

ABSTRACT

Colorectal cancer (CRC) is prone to metastasis, leading to a poor prognosis. miR-411-3p exhibits a tumor-suppressive function in CRC, but its exact mechanism is unclear. The malignant biological properties of CRC cells were detected by Carboxyfluorescein diacetate succinimidyl ester (CFSE) staining, scratch-wound and transwell assay. Levels of markers associated with macrophage polarization were evaluated by flow cytometry and ELISA kits. Bioinformatics analysis to screen whether the downstream target mRNA of miR-411-3p is matrix metalloproteinase 7 (MMP7), and Dual-Luciferase reporter assay verified the targeting relationship between the two. qRT-PCR tested miR-411-3p and MMP7 levels. MMP7 level was quantified by Western blot. Additionally, a nude mouse subcutaneous graft tumor model was constructed, Ki-67 expression was detected by immunohistochemistry, and the impact of miR-411-3p/MMP7 on the polarization of M2 macrophages was explored. miR-411-3p expression is downregulated in CRC. Knockdown of miR-411-3p elevated the amount of CFSE-positive, migrating, and invading cells, decreased apoptosis, and elevated the levels of M2 macrophage polarization markers. After overexpression of miR-411-3p, all of the above metrics were reversed in CRC cells. miR-411-3p targeted negative regulation of MMP7 expression, and MMP7 overexpression further enhanced the promotional effect of knockdown of miR-411-3p on the malignant progression of CRC and M2 macrophage polarization. Furthermore, knockdown of miR-411-3p upregulated the MMP7 level, elevated Ki-67-positive cells count, and induced M2 macrophage polarization *in vivo*. Knockdown of miR-411-3p upregulates MMP7 and induces M2 macrophage polarization, which in turn promotes malignant biological progression of CRC.

Key words: colorectal cancer; miR-411-3p; matrix metalloproteinase 7; M2 macrophage polarization.

Correspondence: Shangkun Du, Department of Gastrointestinal Surgery, Affiliated Hospital of Hebei University, 212 Yuhua East Road, Baoding 071000, Hebei Province, China. E-mail: ShangkunDuShang@hotmail.com

Contributions: TB, PL, developed and planned the study, performed experiments, and interpreted results, edited and refined the manuscript with a focus on critical intellectual contributions; YL, BC, GL, WW, RY, XZ, participated in collecting, assessing, and interpreting the data, and made significant contributions to data interpretation and manuscript preparation; SD, provided substantial intellectual input during the drafting and revision of the manuscript. The final version of the manuscript has been reviewed and approved by all authors.

Conflict of interest: the authors declare no conflict of interest regarding the present study.

Ethics approval: the Ethics Committee at Affiliated Hospital of Hebei University granted approval for the study (No. HDFYLL-KY-2023-043). Every participant provided informed consent for the collection of samples.

Availability of data and materials: the data used to support the findings of this study are available from the corresponding author upon reasonable request.

Funding: 2024 Hebei Province Medical Science Research Project Plan (No. 20241062; President's Fund of Hebei University (No. School 20220036); Hospital Foundation of the Affiliated Hospital of Hebei University (No. 2022QC32); Baoding Science and Technology Plan (No. 2241ZF297); the Natural Scientific Foundation of Hebei Province (No. H2021206177); Hebei Provincial Department of Science and Technology (No. 22377759D).

Introduction

Colorectal cancer (CRC) is one of the most common gastrointestinal tumours, ranks as the third most prevalent tumour globally.[1,2] According to statistics, there were 152,810 new diagnoses and more than 53,000 fatalities in the USA in 2024.[3] The development of CRC involves various elements, such as family genetics, unhealthy eating habits, inflammatory bowel disease, and the living environment.[4,5] In CRC patients, metastasis represents the primary factor contributing to mortality, with around 20% of individuals exhibiting metastases at the time of diagnosis, primarily involving the liver and lungs.[6,7] Currently, common therapeutic approaches for CRC include radiotherapy, surgery, and chemotherapy, with surgery being the management of choice for patients with early stage CRC.[8,9] With the development of technology and the effective combination of multiple therapies, the systemic treatment of patients with metastatic CRC has improved, but their prognosis remains not optimistic, as indicated by a five-year survival rate of only 14%.[10,11] The specific mechanisms of CRC progression and metastasis are still unknown; thus, it is essential to elucidate the molecular mechanisms that contribute to CRC development.

The tumor microenvironment (TME) encompasses various stromal cells (including mesenchymal cells, epithelial cells, *etc*.), immune cells, along with non-cellular components infiltrated around the tumor, significantly influencing tumor invasion and metastasis.[12-14] Tumor-associated macrophages (TAMs) are the most enriched immune cells in the TME.[15] Under the influence of tumor-secreted chemokines and growth factors, TAMs polarize into M1 and M2 phenotypes. M1 macrophage polarization is often referred to as classical activation, whereas polarization of M2 macrophages is often referred to as alternative activation.[16] It has been shown that in the presence of interferon (IFN)-γ and lipopolysaccharide (LPS), TAMs polarize to M1 type, whereas upon exposure to interleukin (IL)-13 and IL-4, TAMs polarize to M2-type.[17] Through producing anti-inflammatory substances like IL-10 and Arginase-1 (ARG-1), M2 macrophage polarization can inhibit the inflammatory response in TME, while promoting tumor cell proliferation and metastasis.[18] Therefore, inhibition of macrophage polarization to M2 type may be a promising cure for cancer, providing a new strategy for treating CRC.

Micro RNAs (miRNAs) are endogenous non-coding RNAs of approximately 22-24 nucleotides in length that regulate cell proliferation, differentiation, migration, and invasion.[19,20] miRNAs can act as either oncogenes or tumor suppressor genes, with their abnormal expression contributing to the onset of many cancer types; therefore, miRNAs are also considered as potential diagnostic or prognostic biomarkers.[21,22] Research indicates that overexpression miR-411-3p suppress the proliferation and migration of oral squamous cell carcinoma cells by the modulation of the Nuclear Factor of Activated T cells 5 (NFAT5).[23] Furthermore, in multiple myeloma, miR-411-3p level is declined, and overexpression miR-411-3p decline hypoxia-inducible factor-1α level, which in turn inhibits the malignant progression of multiple myeloma.[24] However, research has yet to explore the impacts of miR-411-3p on the malignant progression of CRC.

We identified matrix metalloproteinase 7 (MMP7) is a downstream target gene of miR-411-3p by bioinformatics analysis. Therefore, this study investigated the impacts of miR-411-3p/MMP7 on the malignant biological behavior of CRC cells and on macrophage polarization. In addition, a nude mice subcutaneous transplantation tumor model was constructed to investigate the influence of miR-411-3p/MMP7 *in vivo*. This research aimed to elucidate the specific mechanism of action of miR-411-3p/MMP7 in regulating the malignant progression of CRC, and to provide new references for CRC diagnosis and targeted therapy.

Materials and Methods

Clinical tissue samples

CRC tissue and adjacent normal tissue samples were obtained from 29 CRC patients admitted to Affiliated Hospital of Hebei University (comprising 11 individuals in stages I+II, and 18 in stages III+IV), which were cleaned and preserved in liquid nitrogen for spare. The mean age of the patients was 57.41, with 13 females and 16 males. All enrolled patients had not received radiotherapy, chemotherapy, tumor immunotherapy, or other related antitumor treatments prior to surgery, and no metastases were detected. The Ethics Committee at Affiliated Hospital of Hebei University granted approval for the study (No. HDFYLL-KY-2023-043), and every participant provided informed consent for the collection of samples.

Cell culture and treatment

Human colon epithelial cells FHC (C1229, negative for mycoplasma) were supplied from Yingwan Biotechnology (Shanghai, China). CRC cell lines LoVo (SNL-070), SW480 (SNL-074), HCT116 (SNL-077), and SW620 (SNL-360) and human monocytic leukemia cells THP-1 (SNL-044) were supplied from Sunncell Biotechnology Co., Ltd. (Wuhan, Hubei, China) and were correctly identified by STR. FHC cells were cultured in FHC cell complete medium (M1018A, Yingwan Biotechnology). THP-1 was cultured in THP-1 cell-specific medium (SNLM-044, Sunncell Biotechnology Co., Ltd.). CRC cell lines were grown in RPMI-1640 medium (11875119, Gibco, Grand Island, NY, USA) containing 1% penicillin and streptomycin (15140122, Gibco), and 10% fetal bovine serum (F0193, Sigma-Aldrich, St. Louis, MO, USA). The fluid change interval was 3 days, with a 1:3 passaging ratio. The temperature was set to 37°C and placed in an environment with saturated humidity and 5% volume CO_2.

miR-411-3p mimics, inhibitors, MMP7 overexpression plasmid (OE-MMP7) and controls (mimics-NC, inhibitors-NC and OE-NC) were synthesized by RiboBio Co., Ltd. (Guangzhou, Guangdong, China). Referring to the instructions of Lipofectamine 3000 (L3000001, Invitrogen, Austin, TX, USA), control and experimental vectors were transfected into CRC cells. Cells continued to be cultured in the incubator for 48 h after transfection, after which RNA was extracted by Trizol reagent (15596026, Invitrogen), and the transfection efficiency was reflected by detecting miR-411-3p and MMP7 levels.

Carboxyfluorescein diacetate succinimidyl ester (CFSE) staining

1 μL of CFSE probe (C1031, Beyotime, Shanghai, China) was added to each millilitre of cell suspension (1×10^6 cells/mL) to give a final content of 5 μM and left to incubate at 37°C for 10 min for labeling. Five times the volume of complete medium was added while mixing, then the cells were centrifuged and rinsed 2 times with PBS to remove unbound CFSE. A small amount of labelled cell suspension was introduced into to a 96-well plate and observed under a fluorescence microscope (DM3000, Leica, Heidelberg, Germany) to confirm the successful labeling. CRC cells that were successfully pre-stained with CFSE were taken for transfection for 48 h. Subsequently, the cells were transferred to a flow-cytometer tube, and the CFSE fluorescence intensity was detected by flow cytometry (BD FACSCalibur™, BD biosciences, San Jose, CA, USA) with an excitation wavelength of 488 nm.[25]

Transwell assay

Matrigel (HY-K6002, MedChemExpress, Monmouth Junction, NJ, USA) was melted in a refrigerator at 4°C overnight away from light, and subsequently mixed with serum-free RPMI-1640 medium. Transwell chambers (8 μm, Corning, Tewksbury, MA, USA) were placed into 24-well plates, the above dilution gel (100 μL) was pipetted and spread on the bottom of each chamber and placed in the incubator overnight. The following day, the remaining liquid in the chambers was aspirated. Cell suspension (200 μL, 1.5×10^5 cells/mL) was seed into the upper section, followed by the addition of the complete medium in the lower section. Following a 48-h incubation, the cell suspension inside the chambers was discarded, and then exposed to 4% paraformaldehyde (P1110, Solarbio, Beijing, China) for 20 min. Crystal violet (32675, Sigma-Aldrich) was stained for 20 min, subsequently, it was washed twice in PBS. The inner wall cells were scraped off with cotton swabs, and dried naturally in a ventilated place for 2 h. The field of view was randomly selected and captured using microscope (XK-DZ004, SINICO Optical Instrument Co., LTD, Shenzhen, China) to count the amount of invasive cells.

The Transwell migration test does not require treatment of the chambers with Matrigel matrix gel, and the rest of the manipulation and analytical steps are consistent with the invasion test.

Scratch-wound assay

The CRC cells were taken, trypsin-digested, collected, and cell suspension (1 mL, 3×10^5cells/mL) was inoculated into 6-well plates with the horizontal lines drawn in advance. When the cells had completely attached to the wall and grew to more than 80% density, after aspirating and discarding the medium, a 20 μL sterile tip was employed to make a perpendicular scratch at the bottom of the 6-well plate. Subsequently, the cells at the scratch were washed away with PBS, and the wells were filled with serum-free medium. The observation of scratch healing occurred at two time points, 0 h and 48 h. To evaluate the cell migration rate, the widths of scratches were measured utilizing Image J software (version 1.54h, Wayne Resband, National Institute of Mental Health, USA).

Detection of apoptosis by flow cytometry

After various treatments, CRC cells were gathered, rinsed twice with PBS and gently mixed by adding 500 μL Binding Buffer. After that, Annexin-V-APC (5 μL, AP107, MULTI SCIENCE, Hangzhou, Zhejiang, China) and propidium iodide (5 μL) were introduced and left to incubate for 15 min away from light. The cell suspensions were transferred to a flow cytometer for the detection and analysis of cell mortality by FlowJo software (v10.8, BD biosciences).

Preparation of macrophages

Referring to Shao *et al*.,[26] THP-1 cells were treated with PMA (100 ng/mL, HY-18739, MedChemExpress) for 24 h and induced into M0 macrophages. By applying a 48-h treatment with LPS (20 ng/mL, HY-D1056, MedChemExpress) and IFN-γ (20 ng/mL, HY-P7025, MedChemExpress), M0 macrophages were induced into M1 macrophages. Or M0 macrophages were treated with interleukin (IL)-4 (20 ng/mL, I4269, Sigma-Aldrich) and IL-13 (20 ng/mL, I1771, Sigma-Aldrich) for 48 h, to induced M2 macrophages. M1/M2 macrophages were incubated with differently treated CRC cells using Transwell (M1/M2 macrophages in the upper chamber, with CRC cells in the base chamber) for 48 h at 37°C.

Detection of macrophage markers to assess polarization status

After co-cultured with CRC cells for 48 h, M1/M2 macrophages were spread in 6-well plates and rinsed once with sterile PBS. Cells were collected after centrifugation and resuspended in sterile PBS to create a cell suspension (1.0×10^7/mL). APC-labelled CD68 antibody (MA5-23616, Invitrogen) and CD206 antibody (17-2061-82, Invitrogen), PE-labelled CD86 antibody (12-0862-82, Invitrogen) and CD163 antibody (12-1631-82, Invitrogen) were added while mixing and left to incubate for 30 min in the dark. The cell suspensions were transferred to the flow cytometer and the results were analysed by Flow-Jo software (v10.8, BD biosciences)

Bioinformatics analysis

Screening by GEPIA (http://gepia.cancer-pku.cn/), miRDB (https://mirdb.org/index.html) and Home-miRWalk (http://mirwalk.umm.uni-heidelberg.de/) databases for downstream target mRNA of miR-411-3p. The results of the screening from the three databases were taken to the intersection, resulting in the MMP7 gene. In addition, the binding sites for miR-411-3p and MMP7 were predicted by TargetScanHuman 8.0 database (https://www.targetscan.org/vert_80/).

Dual-luciferase reporter assay

Based on the methodology of previous studies,[27] the nucleotide sequences of the MMP7 3'UTR, both wild-type (WT) and mutant (MUT), were amplified through PCR using human genomic DNA as a template and subsequently inserted into pmirGLO (Promega, Madison, WI, USA) to construct a luciferase reporter vector. Utilizing the Lipofectamine 3000, MMP7 3'UTR-WT and mimics-NC, MMP7 3'UTR-WT and mimics, MMP7 3'UTR-MUT and mimics-NC, MMP7 3'UTR-MUT and mimics were co-transfected into CRC cells, respectively. Cells were collected after 48 h of incubation and assayed for luciferase activity using the Dual-Lucy Assay Kit (D0010, Solarbio).

Nude mice subcutaneous tumor model

Balb/c nude mice, aged between 4 and 6 weeks, were obtained from Vitalriver (Beijing, China) and housed at a constant temperature of 22°C, 55 to 60% humidity. The facilities were disinfected regularly, and feeding and drinking were performed autonomously. After one week of acclimatization, mice were randomly divided into six groups of five mice each: the inhibitors-NC group, the inhibitors group, the SW480+THP-1+Control group, the SW480+THP-1+IL-4 group, the SW480-inhibitors-NC+THP-1+IL-4 group, and the SW480-inhibitors+THP-1+IL-4 group. In the inhibitors-NC group, SW480 cells (4×10^6) transfected with inhibitors-NC were injected subcutaneously into mice, whereas in the inhibitors group, SW480 cells transfected with inhibitors were injected. Referring to the method of Gong *et al*.,[28] the SW480+THP-1+Control group was composed of SW480 cells (4×10^6) mixed with PMA (100 ng/mL) treated THP-1 cells (1×10^6) and injected subcutaneously into nude mice, and 200 μL of PBS was injected intraperitoneally into nude mice. The SW480+THP-1+IL-4 group was injected subcutaneously into nude mice by mixing SW480 cells with PMA (100 ng/mL) treated THP-1 cells and intraperitoneally injected with IL-4 (200 μL, 10 ng/mL). The SW480-inhibitors-NC+THP-1+IL-4 group was composed of SW480 cells transfected with inhibitors-NC mixed with PMA (100 ng/mL) treated THP-1 cells and injected subcutaneously into nude mice and intraperitoneally with IL-4. The SW480-inhibitors+THP-1+IL-4 group was composed of SW480 cells transfected with inhibitors mixed with PMA (100 ng/mL) treated THP-1 cells and injected subcutaneously into nude mice and intraperitoneally with IL-4. The size of the tumors was detected using vernier calipers on days 7, 14, 21 and 28 post-injection to calculate the tumor volume.

On day 28, mice were killed through cervical dislocation, and the tumors were completely stripped with tissue shears, weighed and photographed to record the tumor mass. The Affiliated Hospital of Hebei University Animal Ethics and Welfare Committee granted approval for all mice experiments (No. HDFYLL-KY-2023-043), and experiments were followed the Code of Ethics for Laboratory Animals.

qRT-PCR

To isolate total RNA, different cells and tissues were lysed using Trizol reagent. AMV reverse transcriptase (2621, Takara, Tokyo, Japan) was added to obtain cDNA. The target gene was amplified using TB Green FAST qPCR kit (CN830S, TAKARA) and ABI PRISM 7300 RT-PCR system (7300, ABI, Carlsbad, CA, USA), referring to the instructions, with the cDNA as a template. U6 and GAPDH serving as internal controls, and the relative levels of target genes were determined by $2^{-\Delta\Delta Ct}$ method. The primer sequences for the examined genes were: miR-411-3p: F: 5'-ACTTGGAGAGATAGTAGACCGT-3'; R: 5'-ACTGAGGGTTAGTGGACCGT-3'. U6: F: 5'-TGGGGTCAGGAATA GGGAGG-3'; R: 5'-GTTTGCCACGTGCAACTCAT-3'. MMP7: F: 5'-TGCCTTTGGTTCCTGTGAAT-3'; R: 5'-GAATGTCCCAGTCGTACCCC-3'. CD86: F: 5'-TCCAGGCACTGTGCTAAACAT-3'; R: 5'-ACTAGCTCAAAACCCTGGCA-3'. induced NO synthase (iNOS): F: 5'-CAGCATGAGCCCCTTCATCA-3'; R: 5'-TGAAGTCTGTGTCCGAAGGC-3'. IL-1β: F: 5'-AGCCATTTCACTGGCGA-3'; R: 5'-GTAGCCGTCATGGGGAAGTC-3'. Tumor necrosis factor-α (TNF-α): F: 5'-GAGACAGATGTGGGGTGTGAG-3'; R: 5'-TCCTAGCCCTCCAAGTTCCA-3'. CD206: F: 5'-TACGAGGCCATTGGAAGCTC-3'; R: 5'-TTTGGGCTGGTACTGGCTTT-3'. IL-10: F: 5'-CCCTGCAATCAGGAAGCAGA-3'; R: 5'-AGGGCATCAAAAAGACCGCA-3'. ARG-1: F: 5'-ACCTGAAACCAAGTCCCAGC-3'; R: 5'-CGAGCAAGTCCGAAACAAGC-3'. CD163: F: 5'-ACCTGCACTGGAATTAGCCC-3'; R: 5'-CTTGCTCTTTGCGACCTTGG-3'. GAPDH: F: 5'-TGTAGGCTCATTTGCAGGGG-3'; R: 5'-TCCCATTCCCCAGCTCTCTCAT-3'.

Western blot

To obtain proteins, RIPA lysis buffer (P0013B, Beyotime) was utilized for lysing different treated cells or tissues. BCA protein concentration assay kit (P0012, Beyotime) was for assessing the protein content. Next, sample proteins underwent electrophoresis on SDS-PAGE gels (12%, Invitrogen), and shifted to a PVDF membranes (Invitrogen), followed by blocking with 5% skimmed milk for 3 h. After rinsing, the membranes were incubated with MMP7 primary antibody (HY-P81117, 1:1000, MedChemExpress) overnight at 4°C. On the second day, after being rinsed thrice, the membranes were incubated with sheep anti-rabbit secondary IgG (31460, 1:10000, Invitrogen) for 2 h. The chemiluminescent agent ECL (HY-K1005, MedChemExpress) was evenly dripped onto the membrane and scanned with a gel imaging system (iBright CL1500, Invitrogen). Bands were analyzed in gray value using Image J software, and the relative expression was expressed as its ratio to GAPDH (PA1-987, 1:1000, Invitrogen).

Immunohistochemistry

Nude mice tumour tissues were exposed to 4% paraformaldehyde for 24 h at 4°C, routinely dehydrated, sectioned after paraffin embedding (thickness of 4~5 μm), deparaffinized with xylene (247642, Sigma-Aldrich), and placed in 0.1 mol/L citric acid solution (pH=6) for microwave antigen retrieval. Sections were exposed to 3% H_2O_2 solution for 25 min to block endogenous peroxidase. Subsequently, the tissues were evenly covered with drops of 5% bovine serum albumin (BSA, HY-D0842, MedChemExpress), and closed for 30 min. Anti-Ki-67 antibody (PA5-114437, 1:1000, Invitrogen) was gently added and incubated for 90 min at 37°C. As a negative control, primary antibody was omitted and replaced by PBS. Then, samples were covered with HRP-labeled goat anti-rabbit IgG (31460, 1:10000, Invitrogen) for 20 min at 37°C and DAB (DA1010, Solarbio) was used for color development. Nuclei were counterstained with Mayer hematoxylin (MHS16, Sigma-Aldrich) and the slides were sealed with neutral gum. The number of immunopositive (yellow- or tan-stained) cells was counted under a microscope (40×) using Image J software; 5 fields of view were taken from each section.

Immunofluorescence

Paraffin sections were deparaffinized, subjected to antigenic retrieval, and permeabilized with drops of 0.3% Triton X-100 (X100, Sigma-Aldrich) for 10 min. The sections were evenly covered with drops of 5% BSA for 30 min, then placed at 4°C for an

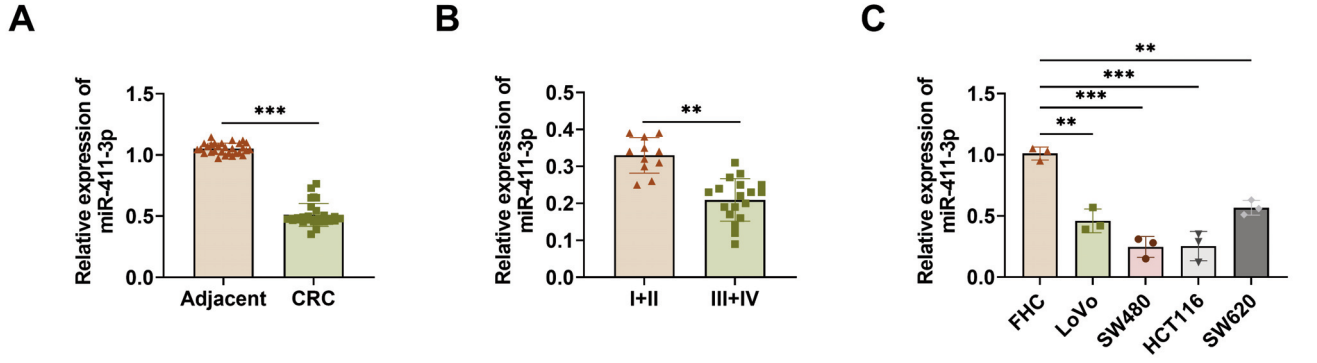

Figure 1. miR-411-3p expression of in CRC. **A**) miR-411-3p level in adjacent tissues and CRC tissues (n=29) was detected through qRT-PCR. **B**) miR-411-3p level in cancer tissues of stage I+II (n=11) and stage III+IV (n=18) CRC patients. **C**) miR-411-3p level in normal colon epithelial cells (FHC) and CRC cell lines (SW480, LoVo, SW620 and HCT116), n=3. **p<0.01, ***p<0.001.

overnight incubation with anti-CD206 antibody (PA5-101657, 1:100, Invitrogen), or anti-CD163 antibody (MA5-54106, 1:1000, Invitrogen). As a negative control, primary antibody was omitted and replaced by PBS. On the following day, the sections were exposed to FITC-labeled goat anti-rabbit IgG secondary antibody (F-2765, 1:200, Invitrogen) in darkness for 1 h at room temperature. Finally, the sections were counterstained with DAPI solution (C1005, Beyotime) for 10 min, and observed under a fluorescence microscope (40×). 5 fields of view were taken from each section, the fluorescence intensity of CD206 or CD163 in the sections were obtained after processing the images with Image J software.

ELISA

Human iNOS (ml061044, Enzyme-linked Biotechnology, Shanghai, China), human IFN-γ (PI511, Beyotime) and human TNF-α ELISA Kit (PT518, Beyotime) were used to assess M1 macrophage polarization. Human IL-10 (ml064299, Enzyme-linked Biotechnology), human ARG-1 (D711111, Sangon Biotech Co., Ltd., Shanghai, China), murine IL-10 (ml059775, Enzyme-linked Biotechnology) and murine ARG-1 ELISA Kit (D721223, Sangon Biotech Co., Ltd.) to assess M2 macrophage polarization. The cell culture or tissue homogenate supernatants were injected into ELISA well plates and incubated for 2 h; after 1-h incubation with the corresponding antibody and 3-times rinsing with the washing buffer, streptavidin-HRP was added for 30 min. Then substrate A and B solution was added and left to incubate for 10 min, followed by the termination solution, and the OD_{450} values were measured immediately through microplate reader (1410101, Thermo Fisher Scientific, Waltham, MA, USA).

Statistical analysis

A minimum of 3 repetitions in each experiment, with the result being reported as the average value ± SD. For statistical analysis of data, we employed SPSS 26.0 software (IBM SPSS Statistics 26). One-way analysis of variance was utilized to conduct multiple comparisons among the groups. In cases of independent samples, Student's *t*-test was utilized if normally distributed, otherwise, non-parametric tests were utilized, with $p<0.05$ representing a significant difference. Plotting was done using Prism software (Graphpad 9.0).

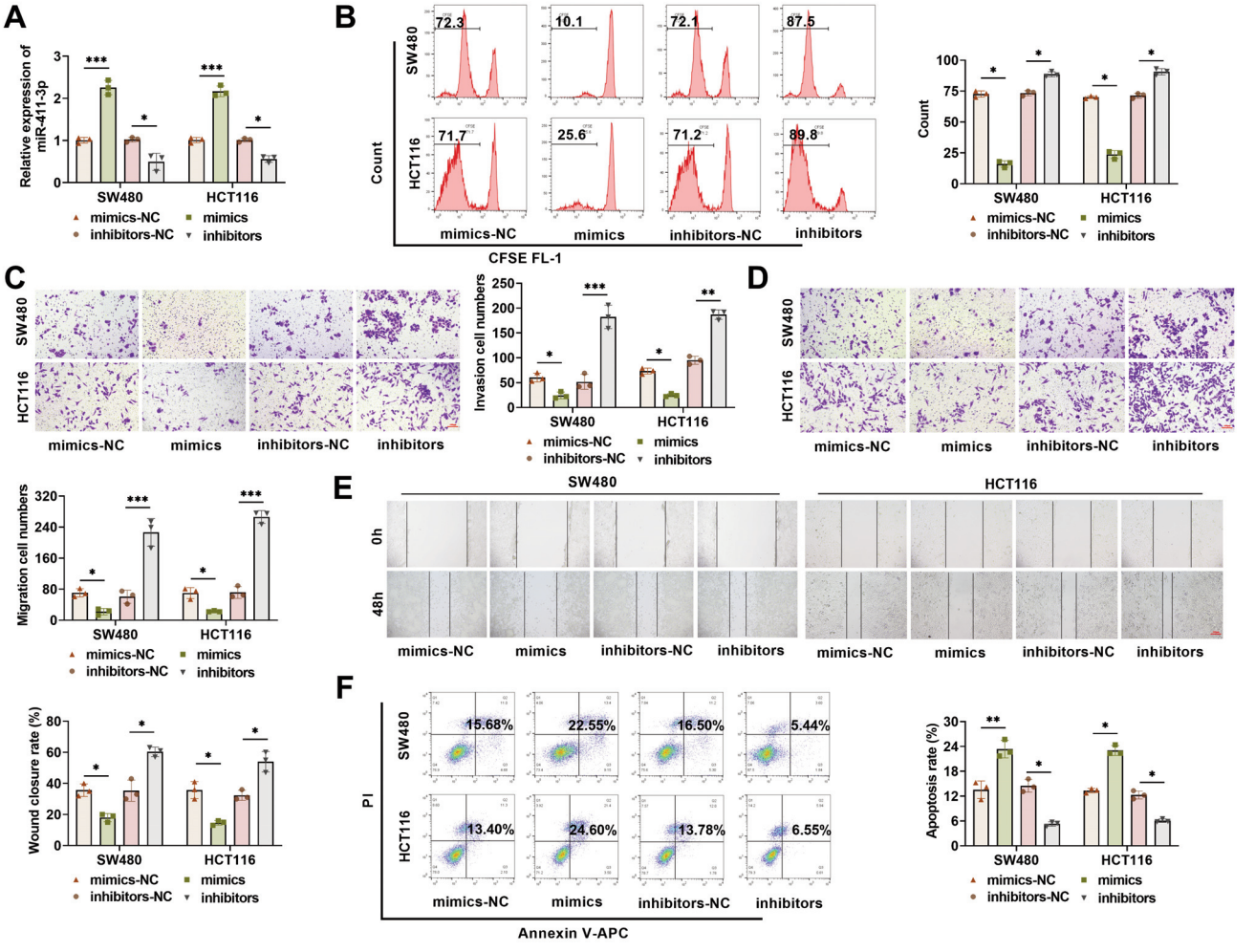

Figure 2. Knockdown miR-411-3p promotes malignant progression in CRC cells. **A**) The mimics and inhibitors were transfected in CRC cells, and miR-411-3p level was assessed via qRT-PCR. **B**) CFSE probe was utilized to evaluate CRC cell proliferation after transfection. **C,D**) The number of invasion and migration of SW480 and HCT116 cells was determined by Transwell assay; magnification 20×; scale bar: 100 μm. **E**) Scratch-wound assay o detect cell migration rate; magnification 20×; scale bar: 100 μm. **F**) Flow cytometry was utilized to evaluate apoptosis rate. *$p<0.05$, **$p<0.01$, ***$p<0.001$.

Results

miR-411-3p is downregulated in CRC

The level of miR-411-3p in adjacent tissues and CRC tissues was tested through qRT-PCR. The findings revealed that miR-411-3p level in CRC was markedly lower than in normal (Figure 1A). Notably, miR-411-3p level was elevated in cancer tissues from CRC patients with stage I and II (n=11) compared to those with stage III and IV (n=18), indicating a potential association between reduced miR-411-3p level and CRC severity (Figure 1B). In addition, we examined miR-411-3p level in normal colonic epithelial cells (FHC) and CRC cells. miR-411-3p level in CRC cells (LoVo, SW480, HCT116, and SW620) was notably lower than in FHC cells, and miR-411-3p level was the lowest in HCT116 and SW480 cells (Figure 1C). Overall, miR-411-3p may act as a tumor suppressor in CRC, prompting the choice of SW480 and HCT116 cells for further investigation.

Knockdown of miR-411-3p promotes CRC malignant biological properties

We transfected mimics/mimics-NC as well as inhibitors/inhibitors-NC in HCT116 and SW480 cells, with their transfection efficiency was verified through qRT-PCR. miR-411-3p level was markedly elevated after transfection with mimics, whereas transfection with inhibitors caused a significant decrease in miR-411-3p level, suggesting that transfection with mimics or inhibitors can effectively regulate miR-411-3p, which can be used for subsequent functional experiments (Figure 2A). By CFSE staining, we observed that overexpression miR-411-3p caused a marked decline in CFSE-positive cell counts, indicating that the cell proliferation was inhibited, whereas knockdown miR-411-3p promoted proliferation of CRC cells (Figure 2B). By Transwell assay, the amount of invasion and migration cells was markedly reduced after miR-411-3p overexpression, but knockdown of miR-411-3p promoted cell invasion and migration (Figure 2 C,D). Scratch assay similarly demonstrated that the scratch healing rate was notably declined after miR-411-3p was overexpressed, with

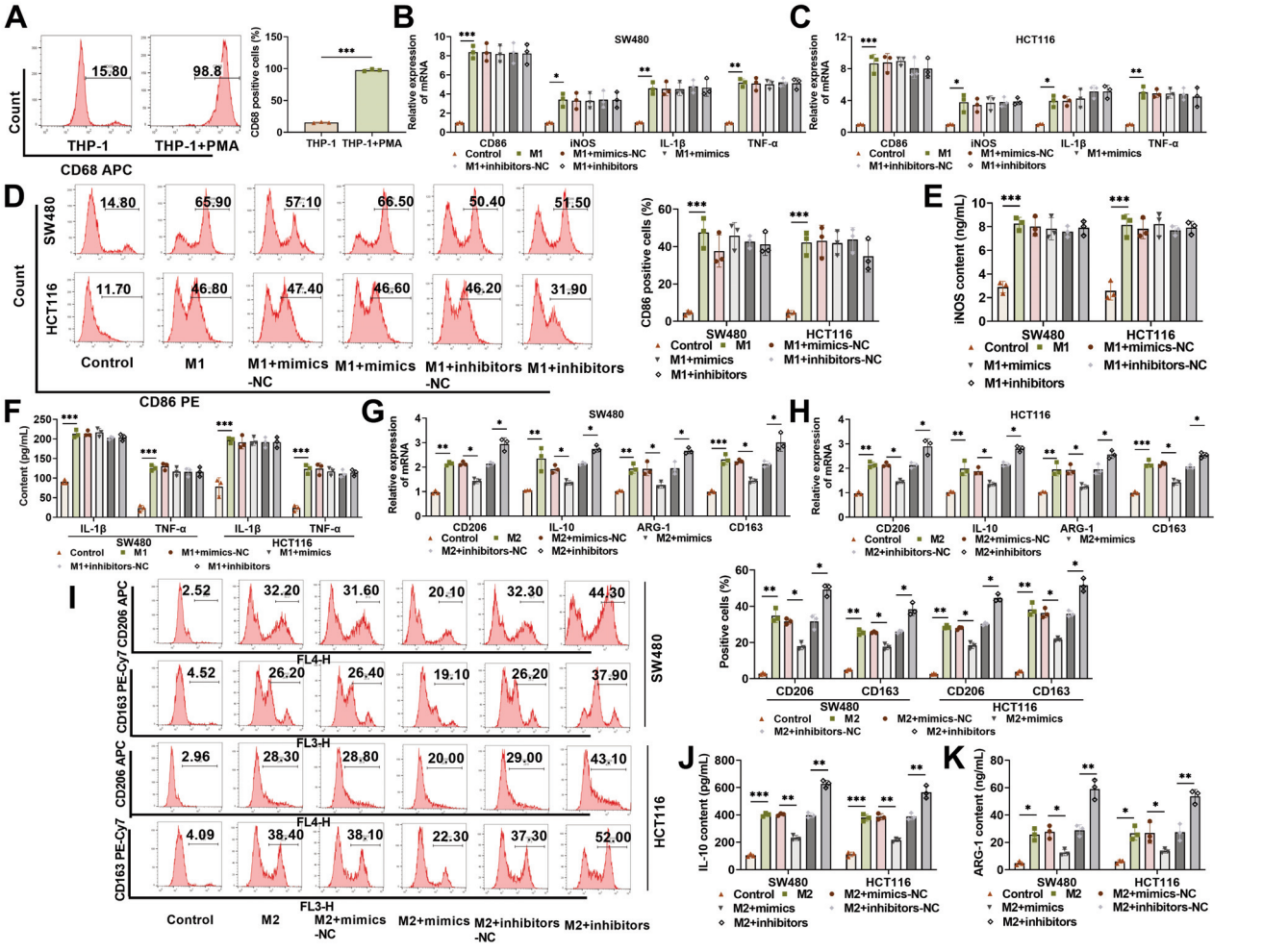

Figure 3. Knockdown miR-411-3p induces M2 macrophage polarization. **A**) M0 macrophage marker CD68 level was assessed by flow cytometry. **B,C**) M0 macrophages were induced into M1 macrophages or M2, and CRC cells were co-cultured with M1 macrophages for 48 h; utilizing qRT-PCR to evaluate M1 macrophage polarization markers levels, like CD86, iNOS, IL-1β and TNF-α. **D**) M1 macrophage marker CD86 level was determined by flow cytometry. **E,F**) M1 macrophage markers (iNOS, IL-1β, and TNF-α) levels were assessed by ELISA. **G,H**) CRC cells were co-cultured with M2 macrophages for 48 h, with CD206, IL-10, ARG-1, and CD163 (M2 macrophage polarization markers) levels were detected by qRT-PCR. **I**) M2 macrophage polarization markers CD206 and CD163 levels were assessed by flow cytometry. J-K) M2 macrophage markers IL-10 and ARG-1 levels were assessed by ELISA. *p<0.05, **p<0.01, ***p<0.001.

knockdown miR-411-3p promoted cell migration (Figure 2E). In addition, flow cytometric results indicated that transfected mimics notably increased the apoptosis rate of SW480 and HCT116 cells, whereas transfection of inhibitors caused a significant decline in apoptosis rate (Figure 2F). The above results findings suggested that after miR-411-3p was overexpressed, the malignant biological behavior of CRC cells was suppressed, while knockdown of miR-411-3p promoted CRC progression.

Knockdown of miR-411-3p induces M2 macrophage polarization

In order to investigate how miR-411-3p affects the malignant behavior of CRC cells, we focused on the process of macrophage polarization. First, to induce THP-1 cells into M0 macrophages, we used PMA stimulation for 24 h and assessed M0 macrophage marker CD68 level through flow cytometry. PMA treatment resulted in a significant increase in CD68-positive cells (up to more than 98%), indicating successful induction of M0 macrophages (Figure 3A). Next, we induced M0 macrophages into M1 macrophages and M2 macrophages, respectively,[29] and co-cultured them with CRC cells for 48 h. In comparison to the control (without added inducing factors), the cells after LPS+IFN-γ induction highly expressed M1 macrophage polarization markers such as CD86, iNOS, IL-1β, and TNF-α, confirming M1 macrophage was successfully induced. Notably, neither overexpression nor knockdown of miR-411-3p had a notable influence on M1 macrophage polarization marker levels (Figure 3 B,C). Flow cytometric and ELISA results also showed no marked changes in CD86, iNOS, IL-1β, and TNF-α levels after co-culturing with CRC cells overexpressing or knocking down miR-411-3p, confirming that miR-411-3p did not affect M1 macrophage polarization (Figure 3 D-F). In addition, cells after IL-4+IL-13 induction highly expressed CD206, IL-10, CD163, and ARG-1 (M2 macrophage polarization markers), confirming successful M2 macrophage induction. Co-cultured with SW480 and HCT116 cells overexpressing miR-411-3p resulted in lower CD206, IL-10, CD163, and ARG-1 levels, whereas knockdown of miR-411-3p resulted in significantly higher levels of these markers, suggesting that knockdown of miR-411-3p induces polarization in M2 macrophages (Figure 3 G-K). These results suggested that miR-411-3p does not affect the polarization process of M1 macrophages, but it does regulate the polarization of M2 macrophages.

Screening and validation of miR-411-3p target genes

Next, we predicted the target mRNAs of miR-411-3p by miRWalk, miRDB and GEPIA databases. Taking the intersection of the three databases, the final target gene obtained was MMP7

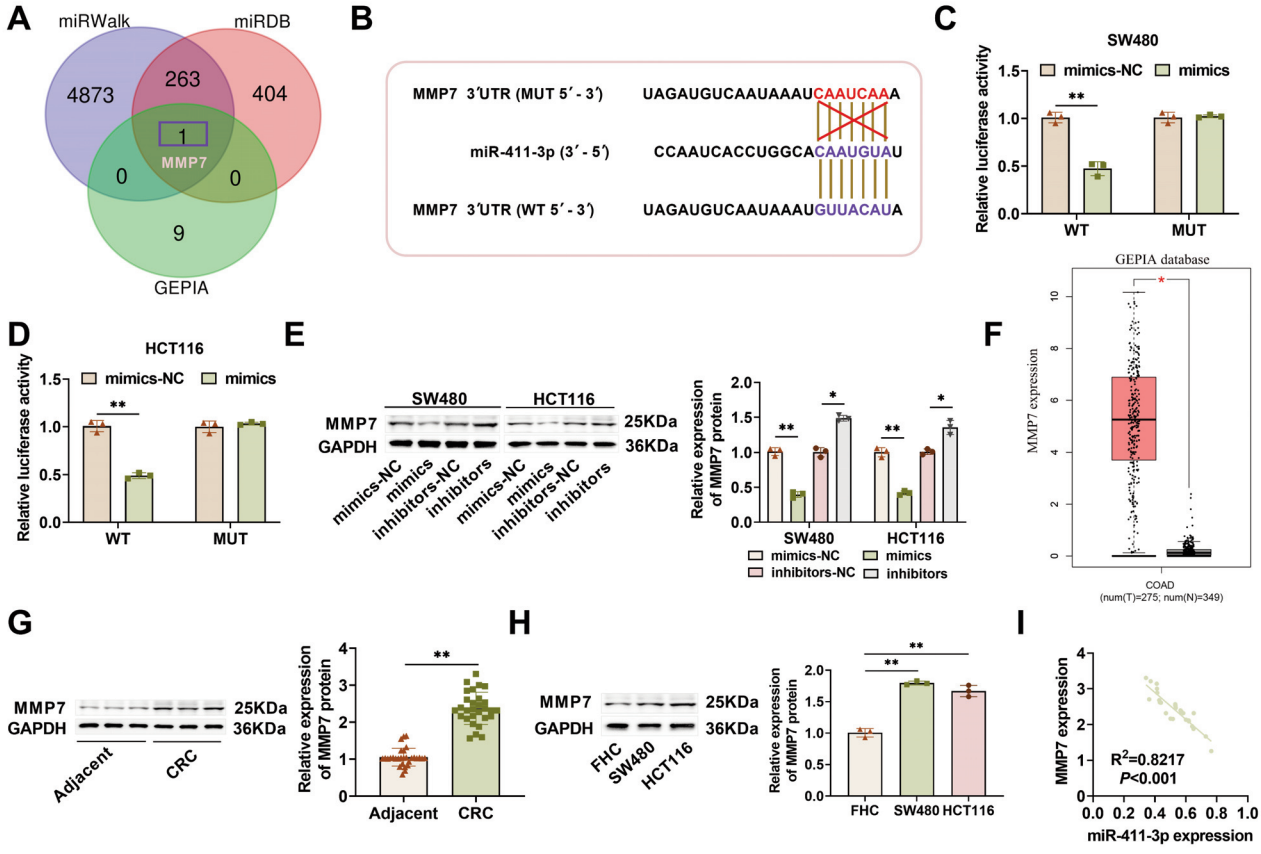

Figure 4. miR-411-3p targets MMP7 and negatively regulates MMP7. **A**) The downstream target genes of miR-411-3p were predicted by GEPIA, miRDB and Home-miRWalk databases, and the MMP7 gene was obtained by taking the intersection of the three. **B**) The sequences of miR-411-3p and MMP7 combined were anticipated by TargetScan database. **C,D**) Dual-luciferase reporter assay verified miR-411-3p can target and regulate MMP7 expression. **E**) Examining MMP7 level in CRC cells through Western blot. F) The GEPIA database revealed an increased level of MMP7 in CRC. **G,H**) Examining MMP7 level in different tissues and cells through Western blot. I) miR-411-3p and MMP7 expression was analyzed by Pearson correlation analysis. *p<0.05, **p<0.01.

(Figure 4A). Subsequently, in the TargetScan database, we identified the binding site of miR-411-3p to MMP7 (Figure 4B). Dual-Luciferase reporter assay demonstrated that over-expression miR-411-3p markedly hindered the luciferase signal of MMP7 WT, with no significant influence on MUT, further confirming that MMP7 is a downstream target gene of miR-411-3p (Figure 4 C,D). Western blot results demonstrated that overexpression miR-411-3p notably declined MMP7 protein level in CRC cells, but knockdown miR-411-3p caused a marked rise in MMP7 levels, confirming that miR-411-3p exerts a negative regulatory effect on MMP7 (Figure 4E). Through GEPIA database, MMP7 level is markedly higher in CRC (Figure 4F). Notably, MMP7 mRNA and protein levels were notably elevated in CRC tissues and cells (SW480 and HCT116) when contrasted with adjacent tissues and FHC cells, a result consistent with the GEPIA database (Figure 4G-4H). In addition, an analysis of Pearson correlation conducted on the relative levels of MMP7 mRNA and miR-411-3p in CRC tissues from patients (n=29) revealed a negative correlation between MMP7 and miR-411-3p levels (Figure 4I). These suggested that miR-411-3p targeted negative regulation of MMP7 expression.

Knockdown of miR-411-3p induces M2 macrophage polarization *via* MMP7 and promotes CRC malignant biological progression

To investigate the impact of overexpression MMP7 on CRC malignant progression, we transfected OE-MMP7 in CRC cells, and MMP7 level was notably elevated after transfection with OE-MMP7 (Figure 5A). Next, for a duration of 48 h, M2 macrophages were co-cultured with CRC cells that had been transfected with inhibitors-NC/inhibitors and OE-NC/OE-MMP7. Knockdown miR-411-3p upregulated CD206 and CD163 levels, elevated IL-10 and ARG-1 levels, and promoted the polarization of M2 macrophages, with overexpression MMP7 further promoted it (Figure 5 B-D). Additionally, overexpression MMP7 further enhanced the promoting impacts of knockdown miR-411-3p on cell proliferation, migration and invasion (Figure 5 E-H). Not only that, knockdown miR-411-3p notably reduced the apoptosis rate of CRC cells, and overexpression MMP7 further inhibited apoptosis (Figure 5I). These findings suggested that knockdown miR-411-3p may induce M2 macrophage polarization and promote malignant biological behaviors in CRC cells by upregulating MMP7 expression.

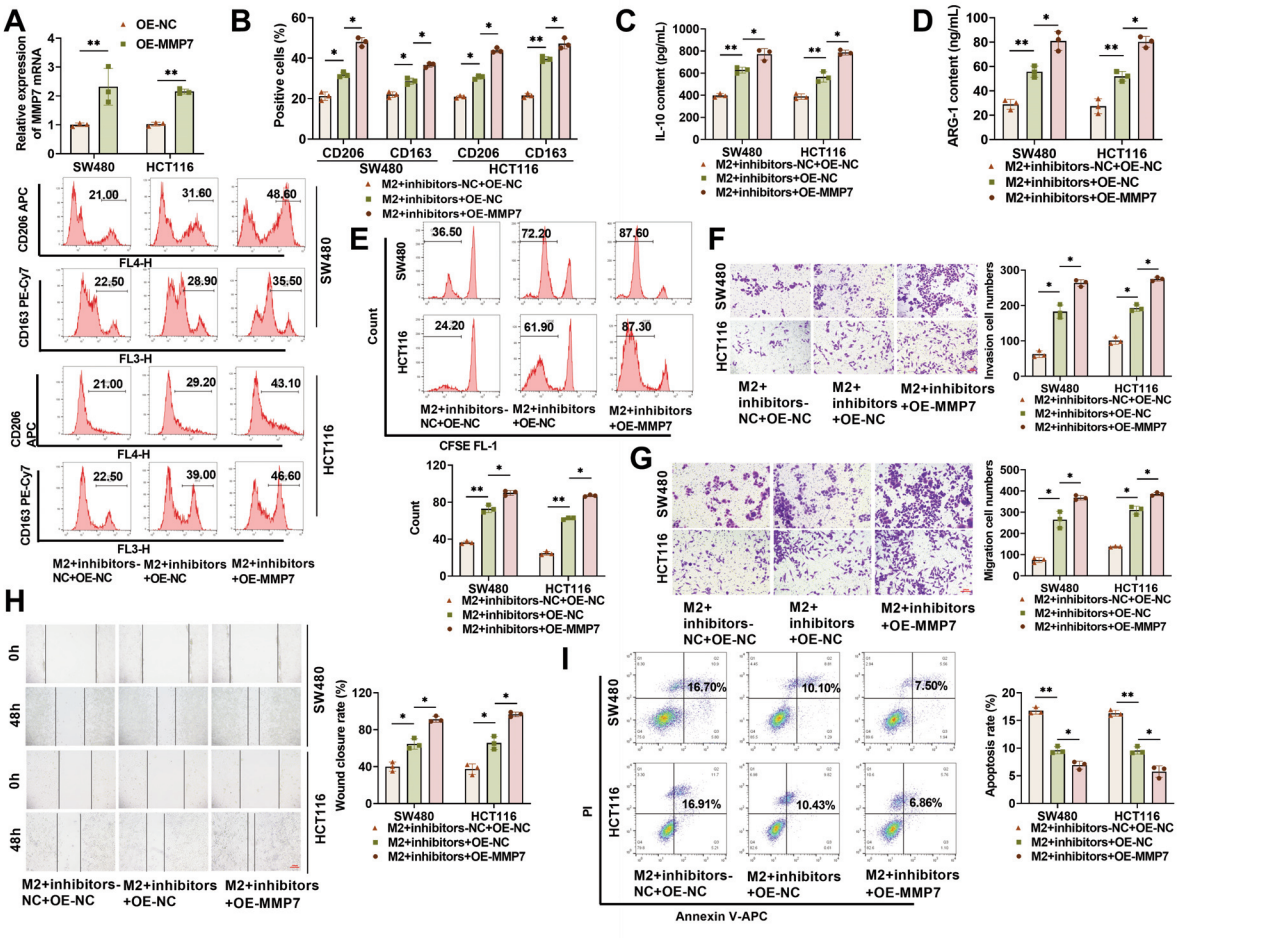

Figure 5. Knockdown miR-411-3p induces M2 macrophage polarization via MMP7 and promotes malignant biological behaviour in CRC cells. **A**) OE-NC and OE-MMP7 were transfected in CRC cells, and the level of MMP7 mRNA was evaluated via qRT-PCR. **B**) After co-cultured with SW480 and HCT116 cells for 48 h, CD206 and CD163 (M2 macrophage polarization markers) levels were detected through flow cytometry. **C,D**) IL-10 and ARG-1 (M2 macrophage markers) levels were evaluated by ELISA. **E**) After co-cultured with M2 macrophages, CFSE probe detected the CRC cell proliferation. **F,G**) After co-cultured with M2 macrophages, the quantity of invasion and migration cells was quantified by Transwell assay; magnification 20×; scale bar: 100 μm. **H**) Scratch-wound assay detected cell migration rate; magnification 20×; scale bar: 100 μm. **I**) The apoptosis rate of CRC was evaluated via flow cytometry. *p<0.05, **p<0.01.

Knockdown of miR-411-3p upregulates MMP7 expression and promotes tumor growth through M2 macrophage polarization

Injection of SW480 cells transfected with inhibitors markedly reduced miR-411-3p level and elevated MMP7 protein level in tumors of nude mice, suggesting that injection of SW480 cells transfected with inhibitors can effectively regulate miR-411-3p and MMP7 levels in tumors (Figure 6 A,B). Compared with SW480+THP-1+Control group, the tumors in nude mice in the SW480+THP-1+IL-4 group were detected to be significantly larger in volume and higher in weight, suggesting that promotion of M2 macrophage polarization promotes tumor growth. Knockdown

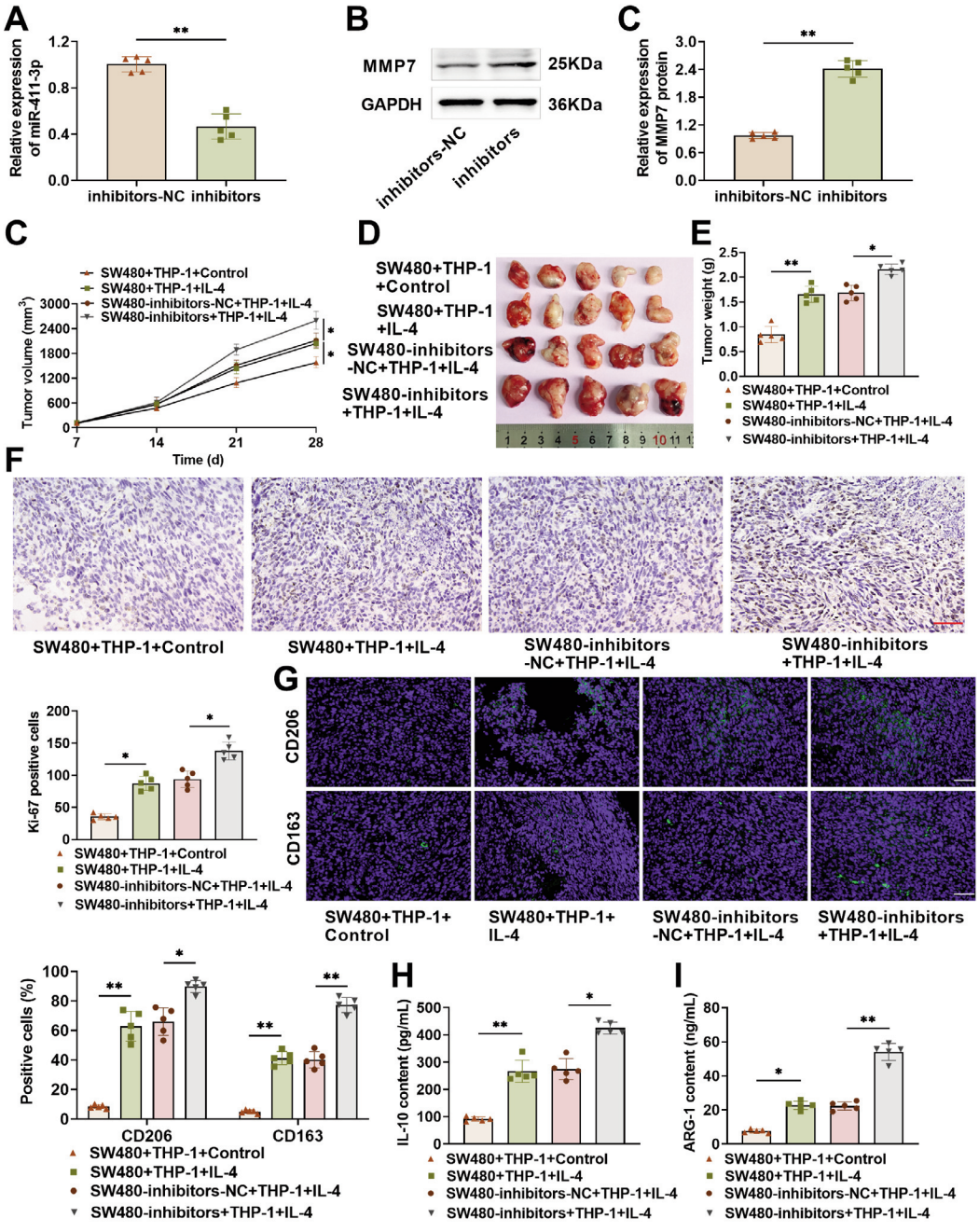

Figure 6. Knockdown miR-411-3p upregulates MMP7 expression and promotes tumor growth through M2 macrophage polarization. **A**) miR-411-3p level in tumor tissues was assessed through qRT-PCR. **B**) Western blot detection of MMP7 level in CRC tissues; SW480 cells were mixed well with THP-1 cells after 24 h of PMA treatment and subcutaneously injected into mice, n=5. C) The size of the subcutaneous tumor was gauged using a vernier caliper on days 7, 14, 21, and 28; at d 28, mice were anesthetized and executed, followed by the removal and imaging of tumors **D**), and tumor weights were recorded (**E**). **F**) Immunohistochemical detection of Ki-67 expression in tumor tissues; magnification 40×, scale bar: 50 μm. **G**) Immunofluorescence detected CD206 and CD163 level in tumor tissues magnification 40×, scale bar: 50 μm. **H,I**) ELISA kit to determine IL-10 and ARG-1 levels in tumor tissues. *p<0.05, **p<0.01.

of miR-411-3p further promoted tumor growth compared with the SW480-inhibitors-NC+THP-1+IL-4 group (Figure 6 C-E). Ki-67 level was significantly elevated in CRC tissues in nude mice in the SW480+THP-1+IL-4 group, and the amount of Ki-67-positive cells was further elevated after knockdown miR-411-3p, suggesting that knockdown miR-411-3p may promote tumor growth by promoting M2 macrophage polarization (Figure 6F). Notably, the amount of CD206- and CD163-positive cells was notably increased in CRC tumor tissues in the SW480+THP-1+IL-4 group, with IL-10 and ARG-1 levels were markedly elevated, and knockdown miR-411-3p further increased the levels of these M2 macrophage polarization markers (Figure 6 G-I). To sum up, knockdown of miR-411-3p could downregulate MMP7 expression and promote M2 macrophage polarization in tumor tissues, which in turn promoted tumor growth.

Discussion

CRC is accounting for about 10% of all new cancer cases, resulting in a significant social burden.[30] Consequently, a deeper comprehension of the underlying mechanisms of malignant progression of CRC is crucial. Our results indicated a low level of miR-411-3p in CRC, and knockdown miR-411-3p promoted malignant biological behaviors in CRC cells, whereas overexpression miR-411-3p did the opposite. Knockdown miR-411-3p induced M2 macrophage polarization but had no significant effect on M1 macrophage polarization. In addition, miR-411-3p targeted and negatively regulated MMP7, and overexpression MMP7 further enhanced the promoting impacts of knockdown miR-411-3p on CRC malignant progression. miR-411-3p may play a key role in CRC malignant progression by acting as a tumor suppressor and interfering with macrophage polarization toward M2 by negatively regulating MMP7. According to the NCBI database (https://www.ncbi.nlm.nih.gov/), miR-411-3p is located on chromosome 14 (14q32.31) and is encoded by the MIR411 gene in the human genome. According to Huang *et al*., the long-chain noncoding RNA PSMA3-AS1 was able to target bind to miR-411-3p, and silencing miR-411-3p caused declined apoptosis and enhanced proliferation in glioma cells.[31] miR-411-3p level was downregulated in ovarian cancer, and knockdown miR-411-3p enhanced malignant progression of ovarian cancer.[3]. In our research, miR-411-3p level was declined in CRC. Notably, miR-411-3p level in cancer tissues from CRC patients with stage III+IV was lower than stage I+II, suggesting the low level of miR-411-3p is closely associated to CRC severity. In cellular functional studies, overexpression miR-411-3p inhibited proliferation, migration and invasion in CRC cells, and knockdown miR-411-3p could promote CRC malignant biological behaviors. These results are similar to previous findings,[31,32] confirming that low level of miR-411-3p promotes the advancement of CRC, and may serve as a valuable indicator for diagnosis and prognosis of tumors.

Immune response is one of the biological properties of TME, acting as a physical barrier to the tumor.[33] Tumors are continuously regulated by immune response mechanisms during tumor development, gradually forming an immunosuppressive microenvironment that mediates tumor immune escape.[6,34] TAMs are currently one of the hotspots in tumor-related research, which can promote tumor cell metastasis through multiple mechanisms,[35] antagonize drug therapy,[36] and are closely related to patient survival time.[37] In CRC, macrophages can interact with intestinal flora to promote colitis and associated tumors.[38,39] Notably, advanced CRC tissues have a large infiltration of M2-type macrophages, which correlates with a negative outcome for patients.[4]. Therefore, both TAMs and tumor cells themselves are important directions for CRC treatment and intervention. CD68 is a marker for M0 macrophages,[41] by stimulating THP-1 cells with PMA, we obtained highly pure M0 macrophages. Using different cytokines,[29] we induced M0 macrophages into the M1 phenotype and M2 phenotype, respectively. Research have demonstrated that miRNAs are crucial in modulating the polarization of TAMs.[42] For example, exosome miR-934 derived from CRC cells induced macrophage polarization to the M2 type, which in turn promotes CRC metastasis to the liver.[43] In our research, no marked alterations in M1 macrophage polarization markers levels were observed after co-culture with CRC cells overexpressing or knocking down miR-411-3p, suggesting that it does not affect M1 macrophage polarization. Whereas overexpression miR-411-3p resulted in notably lower levels of M2 macrophage polarization markers, knockdown of miR-411-3p resulted in higher levels of these markers, suggesting that miR-411-3p regulates M2 macrophage polarization.

Increasing evidence suggested that miRNAs lead to degradation of target gene mRNAs or inhibition of their translation mainly by binding to complementary sequences in the 3'-UTR of mRNAs, which may be the main mechanism by which miRNAs regulate cancer progression.[44,45] By bioinformatics analysis, MMP7 was found to serve as a downstream target gene of miR-411-3p. MMP7 is the smallest secreted matrix metalloproteinase and is vital in immunity, cell differentiation, extracellular matrix degradation, wound healing and angiogenesis.[46,47] According to Hua *et al*., MMP7 expression was elevated in patients with colitis and was closely linked to immune infiltration.[48] MMP7 expression is abnormally elevated in activated M2 macrophages.. Not only that, aberrant expression of MMP7 can affect cancer cell growth and is linked to invasion and recurrence of various malignant tumors.[50,51] Notably, MMP-7 can achieve tumor-promoting or tumor-suppressing effects by regulating multiple complex mechanisms in the TME.[52] A research indicates that MMP7 level in CRC tissues was markedly elevated compared to those in healthy tissues, and upregulation of MMP7 promoted CRC cell metastasis and invasion.[53] In addition, elevated MMP7 level is linked to chemotherapy resistance and unfavorable outcomes in CRC patients, suggesting it could be a valuable biomarker for CRC.[54,55] We discovered that MMP7 was markedly elevated in CRC, which was consistent with previous findings.[53] Overexpression miR-411-3p declined MMP7 protein level in CRC cells, but knockdown miR-411-3p caused an increased MMP7 level, suggesting that miR-411-3p negatively regulates MMP7. Overexpression MMP7 further enhanced the promotional effect of knockdown miR-411-3p on CRC malignant progression, while promoting M2 macrophage polarization, confirming that miR-411-3p acts by regulating MMP7.

In summary, knockdown of miR-411-3p upregulates MMP7 and induces macrophage polarization to M2 type, which in turn promotes malignant progression of CRC. Knockdown miR-411-3p promotes the formation of an immunosuppressive microenvironment in CRC and provides a novel molecular mechanism for invasive metastasis of CRC. This study elucidated that miR-411-3p/MMP7 is vital in immune microenvironment of CRC, so targeting miR-411-3p/MMP7 could serve as a promising target for tumor immunotherapy. However, this study has some shortcomings. Tumor development involves multiple signaling pathways, and future in-depth studies are needed to explore how miR-411-3p/MMP7 regulates these signaling pathways. Additionally, the present study suffered from insufficient sample size and did not investigate the influence of MMP-7 alone on M2 macrophage polarization; subsequent studies need to increase the sample size and further investigate the mechanism of action of MMP-7. Furthermore, whether miR-411-3p can also directly affect the proliferation and migration of CRC by targeting other genes is not known, which also needs to be further explored in the future.

References

1. Biller LH, Schrag D. Diagnosis and treatment of metastatic colorectal cancer: a review. JAMA 2021;325:669-85.
2. Fan A, Wang B, Wang X, Nie Y, Fan D, Zhao X, et al. Immunotherapy in colorectal cancer: current achievements and future perspective. Int J Biol Sci 2021;17:3837-49.
3. Siegel RL, Giaquinto AN, Jemal A. Cancer statistics, 2024. CA Cancer J Clin 2024;74:12-49.
4. Li J, Ma X, Chakravarti D, Shalapour S, DePinho RA. Genetic and biological hallmarks of colorectal cancer. Genes Dev 2021;35:787-820.
5. Patel SG, Karlitz JJ, Yen T, Lieu CH, Boland CR. The rising tide of early-onset colorectal cancer: a comprehensive review of epidemiology, clinical features, biology, risk factors, prevention, and early detection. Lancet Gastroenterol Hepatol 2022;7:262-74.
6. Zhao W, Dai S, Yue L, Xu F, Gu J, Dai X, et al. Emerging mechanisms progress of colorectal cancer liver metastasis. Front Endocrinol (Lausanne) 2022;13:1081585.
7. Simsek M, Besiroglu M, Akcakaya A, Topcu A, Yasin AI, Isleyen ZS, et al. Local interventions for colorectal cancer metastases to liver and lung. Ir J Med Sci 2023;192:2635-41.
8. Wang H. MicroRNAs and Apoptosis in Colorectal Cancer. Int J Mol Sci 2020;21:5353.
9. Buccafusca G, Proserpio I, Tralongo AC, Rametta Giuliano S, Tralongo P. Early colorectal cancer: diagnosis, treatment and survivorship care. Crit Rev Oncol Hematol 2019;136:20-30.
10. Leowattana W, Leowattana P, Leowattana T. Systemic treatment for metastatic colorectal cancer. World J Gastroenterol 2023;29:1569-88.
11. Shin AE, Giancotti FG, Rustgi AK. Metastatic colorectal cancer: mechanisms and emerging therapeutics. Trends Pharmacol Sci 2023;44:222-36.
12. Zhang Z, Zeng X, Wu Y, Liu Y, Zhang X, Song Z. Cuproptosis-related risk score predicts prognosis and characterizes the tumor microenvironment in hepatocellular carcinoma. Front Immunol 2022;13:925618.
13. Oura K, Morishita A, Tani J, Masaki T. Tumor immune microenvironment and immunosuppressive therapy in hepatocellular carcinoma: a review. Int J Mol Sci 2021;22:5801.
14. Ashrafizadeh M. Cell death mechanisms in human cancers: molecular pathways, therapy resistance and therapeutic perspective. J Can Biomol Therap 2024;1:17-40.
15. Zhang Q, Sioud M. Tumor-Associated macrophage subsets: shaping polarization and targeting. Int J Mol Sci 2023;24:7493.
16. Boutilier AJ, Elsawa SF. Macrophage polarization states in the tumor microenvironment. Int J Mol Sci 2021;22:6995.
17. Cao J, Liu C. Mechanistic studies of tumor-associated macrophage immunotherapy. Front Immunol 2024;15:1476565.
18. Yunna C, Mengru H, Lei W, Weidong C. Macrophage M1/M2 polarization. Eur J Pharmaco. 2020;877:173090.
19. Liu Y, Yang Y, Wang X, Yin S, Liang B, Zhang Y, et al. Function of microRNA-124 in the pathogenesis of cancer (Review). Int J Onco. 2024;64:6.
20. Zhao R, Zhao D, Zhu X, Li F, Xiong P, Li S, et al. The influence of miR-3149 on the malignancy progression of gastric cancer by negatively regulating CEACAM5. J Cancer Biomolecul Ther 2024;1:1-10.
21. Hill M, Tran N. miRNA interplay: mechanisms and consequences in cancer. Dis Model Mech 2021;14:dmm047662.
22. Ferragut Cardoso AP, Banerjee M, Nail AN, Lykoudi A, States JC. miRNA dysregulation is an emerging modulator of genomic instability. Semin Cancer Biol 2021;76:120-31.
23. Fu SW, Zhang Y, Li S, Shi ZY, Zhao J, He QL. LncRNA TTN-AS1 promotes the progression of oral squamous cell carcinoma via miR-411-3p/NFAT5 axis. Cancer Cell Int 2020;20:415.
24. Wang M, Zhao HY, Zhang JL, Wan DM, Li YM, Jiang ZX. Dysregulation of LncRNA ANRIL mediated by miR-411-3p inhibits the malignant proliferation and tumor stem cell like property of multiple myeloma via hypoxia-inducible factor 1α. Exp Cell Res 2020;396:112280.
25. Niu M, Yi M, Dong B, Luo S, Wu K. Upregulation of STAT1-CCL5 axis is a biomarker of colon cancer and promotes the proliferation of colon cancer cells. Ann Transl Med 2020;8:951.
26. Shao R, Liu C, Xue R, Deng X, Liu L, Song C, et al. Tumor-derived exosomal ENO2 modulates polarization of tumor-associated macrophages through reprogramming glycolysis to promote progression of diffuse large B-cell lymphoma. Int J Biol Sci 2024;20:848-63.
27. Zhou K, Song B, Wei M, Fang J, Xu Y. MiR-145-5p suppresses the proliferation, migration and invasion of gastric cancer epithelial cells via the ANGPT2/NOD_LIKE_RECEPTOR axis. Cancer Cell Int 2020;20:416.
28. Gong Q, Li H, Song J, Lin C. LncRNA LINC01569 promotes M2 macrophage polarization to accelerate hypopharyngeal carcinoma progression through the miR-193a-5p/FADS1 signaling axis. J Cancer 2023;14:1673-88.
29. Cheng Y, Zhong X, Nie X, Gu H, Wu X, Li R, et al. Glycyrrhetinic acid suppresses breast cancer metastasis by inhibiting M2-like macrophage polarization via activating JNK1/2 signaling. Phytomedicine 2023;114:154757.
30. Wang Z, Dan W, Zhang N, Fang J, Yang Y. Colorectal cancer and gut microbiota studies in China. Gut Microbes 2023;15:2236364.
31. Huang T, Chen Y, Zeng Y, Xu C, Huang J, Hu W, et al. Long non-coding RNA PSMA3-AS1 promotes glioma progression through modulating the miR-411-3p/HOXA10 pathway. BMC Cancer 2021;21:844.
32. Wang Y, Huang Y, Liu H, Su D, Luo F, Zhou F. Long noncoding RNA CDKN2B-AS1 interacts with miR-411-3p to regulate ovarian cancer in vitro and in vivo through HIF-1a/VEGF/P38 pathway. Biochem Biophys Res Commun 2019;514:44-50.
33. Allavena P, Sica A, Solinas G, Porta C, Mantovani A. The inflammatory micro-environment in tumor progression: the role of tumor-associated macrophages. Crit Rev Oncol Hematol 2008;66:1-9.
34. Khan SU, Fatima K, Malik F, Kalkavan H, Wani A. Cancer metastasis: Molecular mechanisms and clinical perspectives. Pharmacol Ther 2023;250:108522.
35. Gao J, Liang Y, Wang L. Shaping Polarization of tumor-associated macrophages in cancer immunotherapy. Front Immunol 2022;13:888713.
36. Li H, Yang P, Wang J, Zhang J, Ma Q, Jiang Y, et al. HLF regulates ferroptosis, development and chemoresistance of triple-negative breast cancer by activating tumor cell-macrophage crosstalk. J Hematol Oncol 2022;15:2.
37. Li H, Miao Y, Zhong L, Feng S, Xu Y, Tang L, et al. Identification of TREM2-positive tumor-associated macrophages in esophageal squamous cell carcinoma: implication for poor prognosis and immunotherapy modulation. Front Immunol 2023;14:1162032.
38. Zhang M, Li X, Zhang Q, Yang J, Liu G. Roles of macrophages on ulcerative colitis and colitis-associated colorectal cancer. Front Immunol 2023;14:1103617.
39. Zegarra Ruiz DF, Kim DV, Norwood K, Saldana-Morales FB, Kim M, Ng C, et al. Microbiota manipulation to increase

macrophage IL-10 improves colitis and limits colitis-associated colorectal cancer. Gut Microbes 2022;14:2119054.
40. Liu Q, Yang C, Wang S, Shi D, Wei C, Song J, et al. Wnt5a-induced M2 polarization of tumor-associated macrophages via IL-10 promotes colorectal cancer progression. Cell Commun Signal 2020;18:51.
41. Allison E, Edirimanne S, Matthews J, Fuller SJ. Breast cancer survival outcomes and tumor-associated macrophage markers: a systematic review and meta-analysis. Oncol Ther 2023;11:27-48.
42. Dai S, Xu F, Xu X, Huang T, Wang Y, Wang H, et al. miR-455/GREM1 axis promotes colorectal cancer progression and liver metastasis by affecting PI3K/AKT pathway and inducing M2 macrophage polarization. Cancer Cell Int 2024;24:235.
43. Zhao S, Mi Y, Guan B, Zheng B, Wei P, Gu Y, et al. Tumor-derived exosomal miR-934 induces macrophage M2 polarization to promote liver metastasis of colorectal cancer. J Hematol Oncol 2020;13:156.
44. Liu C, Yu C, Song G, Fan X, Peng S, Zhang S, et al. Comprehensive analysis of miRNA-mRNA regulatory pairs associated with colorectal cancer and the role in tumor immunity. BMC Genomics 2023;24:724.
45. Zhang M, Bai X, Zeng X, Liu J, Liu F, Zhang Z. circRNA-miRNA-mRNA in breast cancer. Clin Chim Acta 2021;523:120-30.
46. Hu Q, Lan J, Liang W, Chen Y, Chen B, Liu Z, et al. MMP7 damages the integrity of the renal tubule epithelium by activating MMP2/9 during ischemia-reperfusion injury. J Mol Histol 2020;51:685-700.
47. Liao HY, Da CM, Liao B, Zhang HH. Roles of matrix metalloproteinase-7 (MMP-7) in cancer. Clin Biochem 2021;92:9-18.
48. Hua R, Qiao G, Chen G, Sun Z, Jia H, Li P, et al. Single-cell RNA-sequencing analysis of colonic lamina propria immune cells reveals the key immune cell-related genes of ulcerative colitis. J Inflamm Res 2023;16:5171-88.
49. Moin ASM, Sathyapalan T, Diboun I, Atkin SL, Butler AE. Identification of macrophage activation-related biomarkers in obese type 2 diabetes that may be indicative of enhanced respiratory risk in COVID-19. Sci Rep 2021;11:6428.
50. Li XF, Aierken AL, Shen L. IPO5 promotes malignant progression of esophageal cancer through activating MMP7. Eur Rev Med Pharmacol Sci 2020;24:4246-54.
51. Meng N, Li Y, Jiang P, Bu X, Ding J, Wang Y, et al. A comprehensive pan-cancer analysis of the tumorigenic role of matrix metallopeptidase 7 (MMP7) across human cancers. Front Oncol 2022;12:916907.
52. Li YY, Zhang LY, Xiang YH, Li D, Zhang J. Matrix metalloproteinases and tissue inhibitors in multiple myeloma: promote or inhibit? Front Oncol 2023;13:1127407.
53. Ou S, Chen H, Wang H, Ye J, Liu H, Tao Y, et al. Fusobacterium nucleatum upregulates MMP7 to promote metastasis-related characteristics of colorectal cancer cell via activating MAPK(JNK)-AP1 axis. J Transl Med 2023;21:704.
54. Zhou Y, Wang L, Zhou F. Clinical significance of MMP7 levels in colorectal cancer patients receiving FOLFOX4 chemotherapy treatment. Int J Gen Med 2023;16:2671-8.
55. Chen L, Ke X. MMP7 as a potential biomarker of colon cancer and its prognostic value by bioinformatics analysis. Medicine (Baltimore) 2021;100:e24953.

Received: 26 December 2024. Accepted: 13 April 2025.

European Journal of Histochemistry 2025; 69:4178
doi:10.4081/ejh.2025.4178